

## First-Principles Theory of Spontaneous-Resistance Anisotropy and Spontaneous Hall Effect in Disordered Ferromagnetic Alloys.

J. BANHART(\*) and H. EBERT(\*\*)

(\*) *Fraunhofer-Institut for Applied Materials Research  
Lesumer Heerstr. 36, D-28717 Bremen, Germany*

(\*\*) *Institute for Physical Chemistry, University of Munich  
Theresienstr. 37, D-80333 München, Germany*

(received 12 April 1995; accepted in final form 9 October 1995)

PACS. 71.20Cf – Metals, semimetals, and alloys.

PACS. 72.15–v – Electronic conduction in metals and alloys.

PACS. 72.15Gd – Galvanomagnetic and other magnetotransport effects.

**Abstract.** – A fully relativistic first-principles theory of the conductivity of disordered magnetic alloys based on the Kubo-Greenwood formalism and the spin-polarised relativistic Korringa-Kohn-Rostoker coherent-potential approximation (SPRKKR-CPA) method is presented. This new approach allows for a treatment of spin-orbit coupling and spin polarisation on an equal footing and to account properly for the reduction in symmetry caused by the simultaneous presence of them that way. Consequently—in contrast to previous approaches—one has access to a parameter-free theoretical description of the spontaneous-resistance anisotropy and the spontaneous Hall resistivity of magnetic alloys. A first application to the system Fe-Ni yields results which are in very satisfying agreement with experiment.

There are a number of interesting phenomena related to impurity scattering in ferromagnetic alloys for which up to now no description from first principles is available. Among these are the spontaneous-resistance (or magnetoresistance) anisotropy (SMA) and the anomalous (or spontaneous) Hall resistivity (AHR) which occur in principle in any ferromagnetic alloy. Note that these effects must not be confused with the field-dependent normal magnetoresistance and Hall effect.

Quantitatively, both effects are expressed by means of the electrical-resistivity (conductivity) tensor  $\rho(\sigma)$  which for cubic systems with the magnetisation along the  $z$ -axis has the form [1]

$$\rho = \sigma^{-1} = \begin{pmatrix} \rho_{\perp} & -\rho_H & 0 \\ \rho_H & \rho_{\perp} & 0 \\ 0 & 0 & \rho_{\parallel} \end{pmatrix}. \quad (1)$$

While  $\varrho_H$  is a direct measure of the AHR, the SMA is expressed by the ratio [1]

$$\frac{\Delta\varrho}{\bar{\varrho}} = \frac{\varrho_{\parallel}(B) - \varrho_{\perp}(B)}{\bar{\varrho}(B)} \Big|_{B \rightarrow 0}, \quad (2)$$

where  $\bar{\varrho} = (1/3)(2\varrho_{\perp} + \varrho_{\parallel})$  and all quantities are determined by extrapolation to a vanishing external magnetic field  $B$ .

To a great extent motivated by the technological importance of the SMA, there have been a large number of corresponding experimental investigations during the last four decades. Among the systems studied, Ni-based alloys received special attention because of the pronounced SMA found for many of them. In particular, the system Fe-Ni shows one of the largest SMA found so far for transition metal systems. The existing experimental SMA data at low temperatures of disordered, polycrystalline Fe-Ni alloys are summarised in fig. 1. Starting with Fe diluted in Ni,  $\Delta\varrho/\bar{\varrho}$  slowly increases with increasing Fe concentration to reach a maximum at about 10 to 20% Fe. Further increase of the Fe content causes the SMA to fall rapidly to very low values.

It was first noted by Smit [2] that the physical origin of the SMA is the spin-orbit interaction. Based on this central assumption several authors developed more and more sophisticated models to describe the SMA in the past [2,3]. However, all these approaches end up with the  $s$ - $d$  picture of electronic conduction [4]. All theories on SMA presented so far are based on the two-current model separating the total current into two distinct contributions coming from electrons of different spin orientation. Spin-orbit coupling, represented by the parameter  $\gamma$ , gives rise to hybridisation of electronic states of different spin character and causes the SMA that way. Using some additional simplifications, Campbell, Fert and Jaoul (CFJ) [3] found for the SMA ratio

$$\frac{\Delta\varrho}{\varrho} = \gamma \left( \frac{\varrho^{\downarrow}}{\varrho^{\uparrow}} - 1 \right), \quad (3)$$

where  $\varrho^{\downarrow(\uparrow)}$  are the resistivities of the two spin subsystems [3,5]. This expression or a refined version of it has been used up to now to discuss corresponding experimental data considering  $\gamma$  as a fitting parameter. However, one has to note that the above expression cannot be used for a rigorous calculation of the SMA—primarily because  $\gamma$  has no clear-cut definition.

A straightforward and rigorous access to galvanomagnetic effects, without using the above approximations or encountering the mentioned problems, is supplied by the Kubo-Greenwood equation for the conductivity tensor  $\sigma$  [6,7]

$$\sigma_{\mu\nu} = \frac{\hbar}{\pi V_{\text{cryst}}} \text{Tr} \langle j_{\mu} \text{Im} G^{+}(E_{\text{F}}) j_{\nu} \text{Im} G^{+}(E_{\text{F}}) \rangle_{\text{conf}}. \quad (4)$$

Here  $G^{+}(E_{\text{F}})$ , representing the electronic structure of the system, is the positive side limit of the single-particle Green function at the Fermi energy  $E_{\text{F}}$ ,  $j_{\mu}$  is the  $\mu$ -th spatial component of the electronic-current operator  $\mathbf{j}$  and  $\langle \dots \rangle_{\text{conf}}$  denotes the atomic-configuration average for a disordered alloy. Equation (4) can be derived from general linear-response theory without any special assumptions for the diagonal components but requires elastic scattering for the Hall conductivity [8].

By determining  $G^{+}$  via the Korringa-Kohn-Rostoker method of band structure calculation in connection with the coherent-potential approximation (KKR-CPA), eq. (4) can be evaluated in a most reliable way. The corresponding expressions for  $\sigma_{\mu\nu}$  for paramagnetic

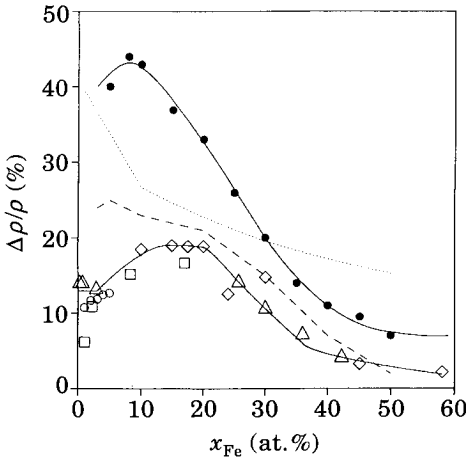


Fig. 1.

Fig. 1. – Spontaneous-resistance anisotropy of Fe-Ni alloys. Open symbols: experimental values at low temperatures ( $\square$ : [1],  $\diamond$ : [2],  $\triangle$ : [3, 9],  $\circ$ : [5]). Full circles: calculated values, broken line: calculated values corrected for extra isotropical scattering; dotted line: SMA calculated by means of eq. (3) (see text). Full lines serve as guides for the eye.

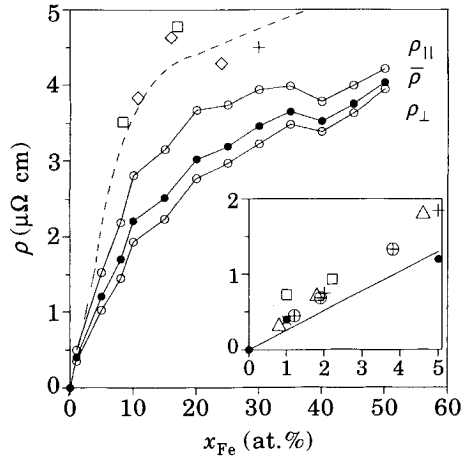


Fig. 2.

Fig. 2. – Calculated residual resistivities of Fe-Ni alloys: longitudinal ( $\parallel$ ) and transverse ( $\perp$ ) resistivity, average  $\bar{\rho} = (1/3)(2\rho_{\perp} + \rho_{\parallel})$ . Experimental low-temperature resistivities  $\bar{\rho}$  by various authors:  $\square$ : [1],  $\diamond$ : [2],  $\times$ : [5],  $\oplus$ : [10],  $+$ : [11],  $\triangle$ : [12]. The solid lines connect calculated values. The dashed line is a guide for the experimental resistivities.

systems and temperature  $T = 0$  K have been derived by Butler [7] and have been applied with great success in their original non-relativistic form [13, 14] as well as their corresponding fully relativistic form [15] to calculate the residual resistivity of various alloy systems.

To get access to the SMA and AHR in the limit  $T = 0$  K we have generalized Butler's approach by evaluating  $G^+$  using the spin-polarized relativistic version of the KKR-CPA (SPRKKR-CPA) [16]. This scheme, based on the Dirac equation for a spin-dependent potential derived from local spin density functional theory, accounts on the same level—without using any parameters—for all relativistic effects as well as for the magnetic state. A natural consequence of this is that the symmetry reduction due to the simultaneous presence of spin-orbit interaction and magnetism—giving rise to the form of  $\boldsymbol{\rho}$  in eq. (1) and that way to the SMA and AHR—is automatically accounted for. This property is completely analogous to that of the conductivity tensor  $\boldsymbol{\sigma}(\omega)$  at finite frequencies  $\omega$  used to discuss magneto-optical phenomena as the Kerr rotation or ellipticity [17]. Finally, one has to mention that using the SPRKKR-CPA there is no need to rely on the two-current model any more.

As a first application of the presented approach we studied the alloy system Fe-Ni in the f.c.c. structure. For various compositions with  $x_{\text{Fe}} \leq 50\%$ , the electronic structure was calculated using the SPRKKR-CPA with an angular-momentum expansion up to  $l_{\text{max}} = 3$ . For each concentration the tensor  $\boldsymbol{\sigma}$  and its inverse  $\boldsymbol{\rho}$  were determined on the basis of eq. (4) taking the so-called vertex corrections into account [7]. The resulting longitudinal and transverse resistivities,  $\rho_{\parallel}$  and  $\rho_{\perp}$ , respectively, together with the average resistivity  $\bar{\rho}$  are shown in fig. 2. Comparison of  $\bar{\rho}$  with experimental values reveals that the calculated resistivities are somewhat lower than the measured ones—especially for higher Fe contents.

This situation is just the same as it is often found when studying the residual resistivity of paramagnetic alloys [14]. The main reason for the discrepancy seems to be that our approach accounts only for chemical disorder but not for topological disorder as the source of the resistivity (see also below).

In full accordance with experiment we find  $\varrho_{\parallel} > \varrho_{\perp}$  for all concentrations of Fe-Ni (see fig. 2). The corresponding positive anisotropy ratio is shown in fig. 1. The most prominent feature of this curve is the very pronounced decrease of  $\Delta\varrho/\bar{\varrho}$  from about 40% for Ni-rich alloys to values of about 7% for 50% Fe. There is even slight evidence for a maximum value at 10% Fe. Obviously, this concentration dependence of the calculated SMA ratio is in rather satisfying agreement with experiment. However, the calculated SMA ratios are about twice as high as the measured ones and the maximum is less pronounced in the calculated curve. There are a number of possible reasons for the observed deviations.

Because of the demanding computational effort, the calculations have been done for a special orientation of the magnetisation  $\mathbf{m}$  ( $\hat{\mathbf{m}} \parallel \hat{\mathbf{z}}$ ), while the experimental data stem from measurements on polycrystalline samples. The dependence of  $\Delta\varrho/\bar{\varrho}$  on  $\hat{\mathbf{m}}$  can be described in terms of the so-called Döring coefficients [1], which have been determined experimentally for  $\text{Fe}_{15}\text{Ni}_{85}$  [18]. From these data we found that the necessary averaging procedure with respect to  $\hat{\mathbf{m}}$  would change the theoretical data by only some few per cent.

A further possible source for the deviation are isotropic contributions to the electrical resistivity which are not included in the calculation and which merely enhance  $\bar{\varrho}$  but not  $\Delta\varrho$ . That such contributions are present is strongly suggested by the results for  $\bar{\varrho}$  in fig. 2. Scattering at grain boundaries, short-range order, clusters etc. could enhance the isotropical resistivity without increasing  $\Delta\varrho$  because this extra scattering is independent of the magnetisation and adds the same  $\varrho_{\text{extra}}$  to  $\varrho_{\parallel}$  and to  $\varrho_{\perp}$ , thus not changing  $\Delta\varrho = \varrho_{\parallel} - \varrho_{\perp}$ . In order to get an idea of how this extra scattering might influence the SMA ratio, we calculated  $\Delta\varrho/\bar{\varrho}$  using experimental values for  $\bar{\varrho}$  instead of the smaller calculated values. The result, shown in fig. 1 as a dashed line, lies much closer to the experimental curve than the uncorrected calculated values.

Finally, from the temperature dependence of  $\Delta\varrho/\bar{\varrho}$  [1] one can expect that extrapolation to  $T = 0$  K will increase the experimental data by around 5%.

Analysis of the matrix element of the current operator in eq. (4) allows one to investigate the role of spin-flip scattering processes for SMA. Within non-relativistic theory these cannot occur because the current operator  $j_{\mu} = -i\hbar(e/m)\nabla_{\mu}$  does not couple to the spin degree of freedom. This differs from the relativistic case where  $j_{\mu}$  is given by  $eca_{\mu}$  with  $a_{\mu}$  one of the Dirac matrices. Analysing the corresponding matrix elements [17], one finds that the spin-flip processes in general contribute to less than 1%. Thus these processes have—at least for  $3d$  systems—practically no influence on the SMA. This confirms the generally made assumption that spin-orbit interaction causes SMA primarily by hybridisation of states of different spin character.

After having calculated the electronic structure of the system Fe-Ni, it is possible to investigate the applicability of the CFJ model for the SMA ratio. In the spirit of this model we set:  $\varrho^{\downarrow}/\varrho^{\uparrow} = n_d^{\downarrow}/n_d^{\uparrow}$ . This implies equal scattering probabilities for all scattering processes from the  $s$ -band and the assumption that the resistivity of each spin subsystem solely arises from  $s$ - $d$  scattering. From the calculations  $\varrho^{\downarrow}/\varrho^{\uparrow}$  is found to decrease continuously from 9 for 1% Fe to 4 for 50% Fe. This agrees quite well with a ratio of 11 deduced from measurements for dilute FeNi [5]. Choosing  $\gamma$  such that  $\Delta\varrho/\varrho = 40\%$  for  $\text{Fe}_1\text{Ni}_{99}$ , one gets a SMA ratio that is given by the dashed line in fig. 1. Obviously, this simple model reproduces the concentration dependence of the SMA ratio only in a very crude way.

Besides the strong SMA, Fe-Ni also exhibits a pronounced AHR. Unfortunately, experimental data over the entire composition range is available only at room temperature.

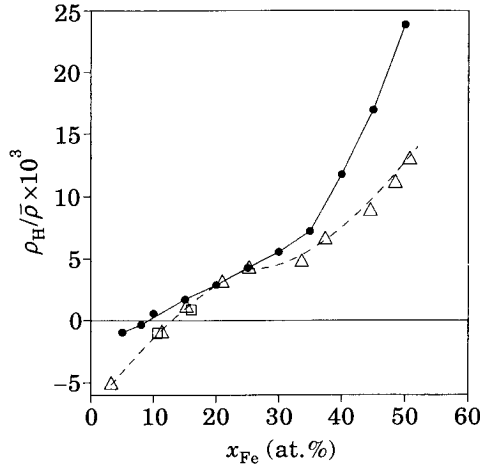


Fig. 3. – Spontaneous Hall angle of Fe-Ni. Full circles: calculated, open symbols: experimental values at room temperature ( $\Delta$ : [19],  $\square$ : [20]).

For this reason, the Hall angle  $\rho_H / \bar{\rho}$  has been plotted in fig.3 to compensate the temperature dependence as far as possible and to allow a comparison to theoretical data for  $T = 0$  K that way. Obviously, the agreement between calculated and measured Hall angles is very satisfactory. The main feature of the data is the change from negative to positive sign upon adding Fe to Ni at about 10% and 14% Fe, respectively. Further increase in Fe content is accompanied by a rapid rise of the Hall angle.

It was already pointed out by Smit [2,20] that the change of sign of the AHR and the maximum value of the SMA occur at roughly the same alloy composition—a feature indeed found by the calculation. This coincidence may be more than accidental, because both phenomena are caused by the presence of spin-orbit interaction. However, the electronic structure does not show any peculiarity for this composition either for the DOS or for the Fermi surface. Furthermore, one should point out that in contrast to the ordinary magneto-resistivity or Hall effect no coupling of an external or internal field to the orbital degree of freedom is needed to give rise to  $\Delta\rho$  or  $\rho_H$ . This is obvious from the Hamiltonian underlying the SPRKKR that contains an exchange-correlation field that couples only to the spin of the electron but contains no term coupling explicitly to the orbital degree of freedom of the electron.

Two distinct scattering mechanisms have been suggested to be responsible for  $\rho_H$ . The skew-scattering mechanism consists in a deflection of the scattered conduction electrons due to the asymmetrical scattering cross-section caused by spin-orbit interactions [20, 21]. The side-jump mechanism proposed by Berger [22] causes a transverse current by a finite lateral displacement of the conduction electrons during scattering. For diluted alloys these sources for  $\rho_H$  are assumed to be given by  $\varphi_{sk} \bar{\rho}$  and  $b_{sj} \bar{\rho}^2$ , respectively. From a corresponding fit of the theoretical data one gets  $\varphi_{sk} = -0.0037$  and  $b_{sj} = 2.0 \text{ n}\Omega\text{cm}$ . This is in reasonable agreement with available experimental data for  $\varphi_{sk}$  ( $-0.00625$  [5] and  $-0.004$  [23]) and  $b_{sj}$  ( $2.25 \text{ n}\Omega\text{cm}$  [5]).

Berger has tried to give an explanation for the change in sign of the AHR in terms of a simple split-band picture of the electronic structure [24]. The Fe- and Ni-related spin-up bands were assumed to be completely filled. Upon increasing the Fe content it is expected that the Fermi energy passes through the top of the Fe- or Ni-related spin-down bands. In contradiction to this, no remarkable shift of the Fermi energy with respect to the Fe or Ni

subbands is found by the calculations. Furthermore, the spin-up bands are not completely filled, thus giving rise to a considerable contribution to the density of states at the Fermi level. Therefore, it seems that no simple explanation for the change in sign of the AHR can be given in terms of the density of states alone.

In conclusion, the fully relativistic spin-polarised KKR-CPA in conjunction with the Kubo-Greenwood theory for electrical conduction allowed for the first rigorous and parameter-free calculation of the SMA ratio and AHR in disordered ferromagnetic alloys. Application to the system Fe-Ni led to very satisfying agreement with experiment. This opens the way for further detailed discussions of experimental data. Furthermore, it will be possible to investigate the fundamental question whether there is an upper limit for the SMA as is suggested by experimental data and other related problems.

## REFERENCES

- [1] MCGUIRE T. R. and POTTER R. I., *IEEE Trans. Mag.*, **11** (1975) 1018.
- [2] SMIT J., *Physica*, **16** (1951) 612.
- [3] CAMPBELL I. A., FERT A. and JAUL O., *J. Phys. C*, **3** (1970) S95.
- [4] MALOZEMOFF A. P., *Phys. Rev. B*, **34** (1986) 1853.
- [5] DORLEIJN J. W. F., *Philips Res. Repts.*, **31** (1976) 287.
- [6] GREENWOOD D. A., *Proc. Phys. Soc. London*, **71** (1958) 585.
- [7] BUTLER W. H., *Phys. Rev. B*, **31** (1985) 3260.
- [8] CHESTER G. V. and THELLUNG A., *Proc. Phys. Soc.*, **73** (1959) 745.
- [9] CAMPBELL I. A., *J. Phys. F*, **4** (1974) L181.
- [10] SCHWERER F. C. and CONROY J. W., *J. Phys. F*, **1** (1971) 877.
- [11] CADEVILLE M. C. and LOEGEL B., *J. Phys. F*, **3** (1973) L115.
- [12] FARRELL T., GREIG D., *J. Phys. F*, **1** (1968) 1359.
- [13] SWIHART J. C., BUTLER W. H., STOCKS G. M., NICHOLSON D. M. and WARD R. C., *Phys. Rev. Lett.*, **57** (1986) 1181.
- [14] BROWN R. H., ALLEN P. B., NICHOLSON D. M. and BUTLER W. H., *Phys. Rev. Lett.*, **62** (1989) 661.
- [15] BANHART J., EBERT H., VOITLÄNDER J. and WEINBERGER P., *Phys. Rev. B*, **50** (1994) 2104.
- [16] EBERT H., DRITTLER B. and AKAI H., *J. Magn. & Magn. Mater.*, **104-107** (1992) 733.
- [17] GUO G.-Y. and EBERT H., *Phys. Rev. B*, **50** (1994) 1037.
- [18] BERGER L. and FRIEDBERG S. A., *Phys. Rev.*, **165** (1968) 670.
- [19] JELLINGHAUS W. and ANDRÉS A. P., *Ann. Phys. (N.Y.)*, **5** (1960) 187.
- [20] SMIT J., *Physica*, **21** (1955) 877.
- [21] FERT A. and JAUL O., *Phys. Rev. Lett.*, **28** (1972) 303.
- [22] BERGER L., *Phys. Rev. B*, **2** (1970) 4559.
- [23] JAUL O., Thesis, Université de Paris-Sud, Centre d'Orsay (1974).
- [24] BERGER L. and BERGMAN G., in *The Hall Effect and its Applications*, edited by C. L. CHIEN and C. R. WESTGATE (Plenum Press, New York, N.Y.) 1980.